Knee Surg Sports Traumatol Arthrosc (2016) 24:2216–2224
DOI 10.1007/s00167-015-3547-2

SHOULDER

Quantitative MRI characterization of arthroscopically verified supraspinatus pathology: comparison of tendon tears, tendinosis and asymptomatic supraspinatus tendons with T2 mapping

Edmund Ganal · Charles P. Ho · Katharine J. Wilson · Rachel K. Surowiec · W. Sean Smith · Grant J. Dornan · Peter J. Millett

Received: 8 October 2014 / Accepted: 18 February 2015 / Published online: 5 March 2015

Abstract
Purpose Quantitative MRI T2 mapping is a non-invasive imaging technique sensitive to biochemical changes, but no studies have evaluated T2 mapping in pathologic rotator cuff tendons. It was sought to evaluate the efficacy of T2 mapping in detecting differences in the supraspinatus tendon (SST) among patients with tendinosis, partial tears and minimally retracted full-thickness tears, relative to asymptomatic volunteers.
Methods The pathologic cohort consisted of two arthroscopically verified groups: tendinosis and a tear group of partial tears or minimally retracted full-thickness tears, and was compared to an asymptomatic cohort with no prior history of shoulder pathology. The SST was manually segmented from the footprint to the medial humeral head in the coronal and sagittal planes and divided into six clinically relevant subregions. Mean T2 values and inter- and intra-rater reliability were assessed.
Results In the anterolateral subregion, the tear group exhibited significantly higher mean T2 values (43.9 ± 12.7 ms) than the tendinosis (34.9 ± 3.9 ms; $p = 0.006$) and asymptomatic (33.6 ± 5.3 ms; $p = 0.015$) groups. In the posterolateral subregion, the tear group had higher mean T2 values (45.2 ± 13.7) than the asymptomatic group (34.7 ± 6.7; $p = 0.012$). Inter- and intra-rater reliability was mostly excellent (ICC > 0.75).
Conclusion T2 mapping is an accurate non-invasive method to identify quantitatively early rotator cuff pathology. The lateral region in the coronal plane in particular may differentiate partial and small minimally retracted full-thickness tears from tendinosis and asymptomatic tendons. Understanding and being able to measure quantitatively the process of tendon degeneration and subsequent tearing may help clinicians to better predict at-risk groups and to stratify treatment options.
Level of evidence III.

Keywords Rotator cuff · Tendinosis · Partial and full tear · Supraspinatus · T2 mapping · MRI

Introduction

Rotator cuff pathology accounts for over 4.5 million physician visits annually [32]. Diagnosis of a rotator cuff tear can often be obtained with a detailed history and physical examination [18], with imaging commonly used to determine specific clinical pathology [4, 17, 31]. In particular, conventional magnetic resonance imaging (MRI) plays a significant role in differentiating tendinosis from partial and full-thickness tears, determining the quality of the tendon, detecting atrophy and fatty degeneration of the muscle, and identifying associated shoulder pathology.

Currently, MRI is the most effective imaging modality in the evaluation of the rotator cuff; however, its diagnostic sensitivity and specificity remain variable [2, 25, 27, 28]. Diagnosis of rotator cuff pathology through MRI is based on qualitative morphology and signal change and becomes increasingly difficult in the presence of partial rotator cuff

E. Ganal · P. J. Millett (✉)
The Steadman Clinic, 181 W Meadow Dr, Suite 400, Vail, CO 81657, USA
e-mail: drmillett@thesteadmanclinic.com

C. P. Ho · K. J. Wilson · R. K. Surowiec · W. S. Smith · G. J. Dornan
Steadman Philippon Research Institute,
181 W Meadow Dr, Vail, CO 81657, USA
e-mail: kwilson@sprivail.org

tears [2, 27–29]. Tendinosis is even more challenging to diagnosis because the morphology is not affected and signal intensity alone has proven unreliable in differentiating between normal and degenerative rotator cuff tendons [5]. A more robust method of quantifying the differences between asymptomatic and damaged rotator cuff tendons is needed to improve MRI diagnosis for treatment planning.

Conventional MRI findings provide information on tendon morphology and tear size but do not allow for earlier detection of tendon degeneration and associated histologic biochemical changes. Quantitative information would be clinically valuable to augment subjective interpretation in the diagnosis of rotator cuff pathology, predict progression of rotator cuff disease, formulate a treatment plan particularly for partial rotator cuff tears and minimally retracted full rotator cuff tears, and assess the outcome of treatment. Novel quantitative biochemical MRI techniques, such as T2 mapping, have been increasingly evaluated for their demonstrated sensitivity in detection of earlier biochemical changes (i.e. collagen fibril structure, orientation, and water content) in various tissues [11–14, 22, 23, 33]. When evaluating the tendon, several studies have demonstrated that the bulk T2 values are multi-exponential and that T2 relaxation times may be feasible to monitor the levels of degeneration and the healing process of collagen structures in the tendon non-invasively [30]. These hypotheses have been corroborated in work performed using T2 mapping in the Achilles tendon and in the asymptomatic supraspinatus tendon [1, 7, 8]. Anz et al. [1] first described T2 mapping for the evaluation of the supraspinatus tendon in asymptomatic individuals and reported excellent inter- and intra-rater reliability. This study demonstrated that T2 values corresponded to the anatomical structure of the muscle–tendon unit with no significant effect due to the ageing process in asymptomatic individuals. However, the effect of earlier degeneration of the supraspinatus tendon on T2 values remains largely unknown.

Before T2 mapping can be implemented into the routine clinical protocol, it is essential that the T2 values of various stages of rotator cuff pathology are documented. As such, the purpose of this prospective study was to evaluate the clinical use of MRI T2 mapping for arthroscopically verified pathologic supraspinatus tendons. Our hypothesis was that there would be differences in T2 values of supraspinatus tendons with non-tear tendinosis and with partial or minimally (slightly) retracted full-thickness tears, compared with asymptomatic supraspinatus tendons. Using the subregions proposed by Anz et al. [1], it was additionally hypothesized that the analysis would yield high inter- and intra-rater reliability measurements in this pathological cohort. The results of this study will help to confirm variability of T2 values, establish T2 values in various stages of rotator cuff pathology, and evaluate how these values differ from a screened asymptomatic cohort, and help clinicians to better predict at-risk groups and to stratify treatment options.

Materials and methods

This study was approved by the institutional review board at (*blinded for review*), and informed consent was obtained from all individual participants included in the study. The asymptomatic cohort was prospectively enrolled and deemed asymptomatic through an injury history questionnaire and verified by a normal physical examination of the shoulder performed by the senior orthopaedic surgeon of this study. The pathologic supraspinatus tendon cohort was prospectively enrolled and consisted of two groups: (1) tendinosis with no tear present and (2) partial or minimally retracted full-thickness tear (combined small tear group) as representing tendon degeneration properties to the point of macroscopic tear/failure. Grossly, retracted tears were not included as the landmarks for defining lateral, middle, and medial subregions, and the criteria for measurements and reproducibility do not apply to a retracted torn tendon. Inclusion criteria for the pathologic cohort included patients who had failed non-operative treatment, had a pre-operative T2 mapping MRI scan performed on the same 3.0 T scanner, and had arthroscopically confirmed supraspinatus pathology by the senior orthopaedic surgeon showing either tendinosis, a partial tear, or a full-thickness minimally (slightly) retracted tear defect of <1 cm (with the proximal stump close to the bony insertion, Patte classification stage 1 [26]). Exclusion criteria for all cohorts included previous surgery on the imaged shoulder or an MR imaging study performed at an outside clinic. Patients with full-thickness tears retracted to the proximal stump at the level of the humeral head (stage 2) or to the proximal stump at the glenoid level (stage 3) were excluded.

Subjects

The asymptomatic cohort consisted of 15 volunteers with a mean age of 39.9 years (range 32–55 years), with 8 males and 7 females. The tendinosis group consisted of 11 patients with a mean age of 45.0 years (range 32–70 years), with 5 male and 6 females. Tendinosis was characterized as a degenerated, frayed, and macerated, but intact tendon with the occurrence of synovitis as well as subacromial bursitis. The tear group consisted of 24 patients (15 partial tears, 9 minimally retracted full-thickness tears) with a mean age of 48.0 years (range 37–72 years), with 14 males and 10 females. Partial thickness tears were defined as incomplete, non-detaching ruptures on either the intra-articular (PASTA: partial articular SSP tendon avulsion) or

the bursal side of the tendon. In the cohort, 9 subjects had articular-sided partial tears (5 were <50 % of the tendon thickness, 4 were greater) and 6 subjects had bursal-sided partial tears (3 were <50 % of the tendon thickness, 3 were greater). Full-thickness minimally retracted tears were defined as fully detached ruptures with the defect from the intra-articular to the subacromial space, and the tendon retracted medially not more than 10 mm.

Image acquisition

All patients and asymptomatic volunteers underwent MR imaging at 3.0 T (Magnetom Verio, Siemens Medical Solutions, Erlangen, Germany) with a gradient strength of 40 mT/m, using a four-channel small shoulder array coil (Invivo, Gainesville, FL, USA). Patients and volunteers were positioned in the supine position with the arm at their side and palm supinated. The scanning protocol consisted of five stages: (1) a proton density-weighted fat-suppressed turbo-spin echo scan in the axial plane (PD-TSE FS Ax), (2) a proton density-weighted fat-suppressed turbo-spin echo scan in the sagittal plane (PD-TSE FS Sag), (3) a proton density-weighted fat-suppressed turbo-spin echo scan in the coronal plane (PD-TSE FS Cor), (4) a multi-echo spin echo T2 mapping scan in the sagittal plane (MESE T2 Map Sag), and (5) a multi-echo spin echo T2 mapping scan in the coronal plane (MESE T2 Map Cor). The details of the scanning parameters are given in Table 1. In the asymptomatic cohort, the axial clinical scan and the raw images from the two T2 mapping scans were reviewed to verify the absence of rotator cuff pathology. T2 mapping values were calculated using a Siemens WIP (work in progress) algorithm which was modified from the Siemens MapIt software algorithm (Siemens Medical Solutions, Erlangen, Germany).

Data analysis

The supraspinatus muscle and tendon were manually segmented as a unit using a stylus and touch screen monitor directly on the second echo of the mapping sequence on a slice-by-slice basis spanning all slices using commercial software (Mimics, Materialise, Plymouth, MI, USA). The muscle tendon unit was evaluated from the footprint to the level of the medial aspect of humeral head in both the coronal and sagittal planes (Fig. 1). The corresponding PD-TSE FS (coronal and sagittal) was simultaneously examined on a neighbouring monitor to aid in the exclusion of synovial fluid and chemical shift artefact in the manual segmentations. In order to evaluate inter- and intra-rater reliability, two raters (a sports medicine orthopaedic surgeon with 6-year experience and a musculoskeletal radiologist with 16-year experience) each segmented the supraspinatus muscle and tendon unit twice in each plane, with a minimum of 30 days observed between segmentations.

To evaluate the presence of variability in T2 values based on the anatomical location within the three groups, the muscle tendon unit segmentation was further divided into six subregions. To perform this subregion division, the raters manually selected two landmarks on the second echo of the MRI T2 mapping image: one on the most lateral aspect of the greater tuberosity and other on the most medial aspect of the humeral head on the coronal (Fig. 1). The coordinates of the manual landmarks were exported, and custom image analysis software (MATLAB, Mathworks, Natick, MA) was used to divide the muscle–tendon unit into thirds based on these landmarks. This provided a reproducible method of creating lateral, middle, and medial subregions for each subject. These three subregions were then further divided into anterior and posterior halves. For the sagittal plane, this was done by dividing the

Table 1 Parameters of the imaging sequences used in the study

Sequence	T2 map sag	T2 map cor	PD-TSE FS cor	PD-TSE FS sag	PD-TSE FS ax
Repetition time (ms)	2000	2000	3000	3000	3350
Echo time (ms)	10.7–74.9	10.7–74.9	46	46	46
Field of view (mm)	140	140	120	120	120
Matrix	256 × 256	256 × 256	256 × 192	256 × 192	256 × 192
Voxel size (mm)	0.5 × 0.5 × 2.0	0.5 × 0.5 × 2.0	0.6 × 0.5 × 3.0	0.6 × 0.5 × 3.0	0.6 × 0.5 × 3.0
Slice thickness (mm)	2	2	3	3	3
Inter-slice gap (mm)	1	1	0	0	0
Number of slices	18	20	25	25	29
Echo trains/slice	–	–	41	41	36
Turbo factor	–	–	8	8	8
Examination time	6:30	6:30	2:11	2:11	2:09

MR parameters for quantitative and morphological imaging

Map mapping, *PD* proton density, *TSE* turbo-spin echo, *FS* fat suppression, *sag* sagittal, *cor* coronal, *ax* axial

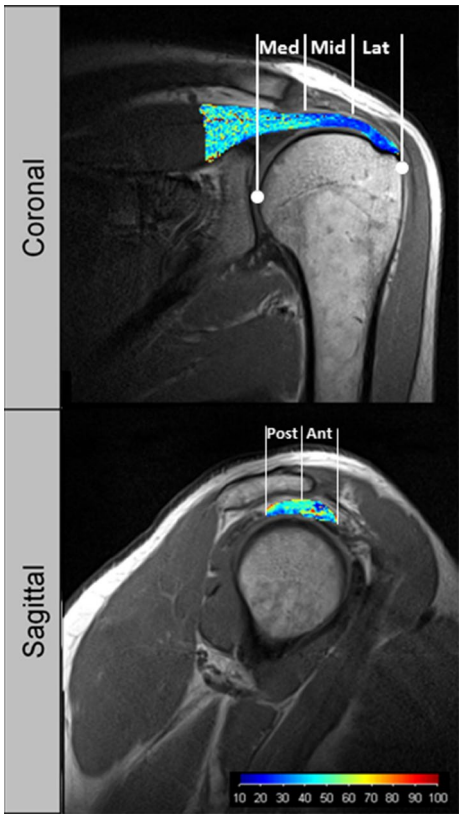

Fig. 1 Evaluation of the supraspinatus muscle tendon unit from the footprint to the glenoid in the coronal and sagittal planes with T2 overlay based on manual segmentations. Coronal image depicts *medial*, *middle*, and *lateral* subregion divisions based on the landmarks placed on the most lateral aspect of the greater tuberosity and the most medial aspect of the humeral head (*white* circles). Sagittal image depicts *posterior* and *anterior* subregion divisions

segmentation into half within each slice (Fig. 1), and for the coronal plane, this was done by dividing which slices were anterior and posterior. This created six subregions in total: anterolateral, posterolateral, anteromiddle, posteromiddle, anteromedial, and posteromedial. Descriptive T2 statistics (mean, standard deviation, minimum, maximum, and number of pixels in each subregion) were calculated within each subregion.

Statistical analysis

A sample size calculation was conducted using T2 data from the first three subjects collected in each group to inform relevant mean and variance estimates. Assuming group standard deviation of 8.0 ms and accounting for multiple comparisons, it was concluded that 14 subjects per group would be sufficient to detect a pairwise group difference in mean T2 values of 10.0 ms with 80 % power. Mean T2 values within each subregion in the two planes were compiled, and pathology groups were compared using a one-way ANOVA for each subregion and viewing plane separately. Equal variances among groups were not assumed; thus, Welch's ANOVA and the Games-Howell method for post hoc pairwise comparisons were used. Additionally, the standard deviation of T2 values within each subregion were compiled and compared in the same manner. Differences between groups with a p value of <0.05 were considered statistically significant. Group summary statistics are reported as mean ± standard deviation.

Intra- and inter-rater reliability was evaluated in a manner that could be generalized to a single future rater from a population of qualified raters using a two-way random effects model to calculate the single measure intraclass correlation coefficient (ICC) for the mean T2 value within each subregion. The ICC values were graded using the scale described by Fleiss et al. [6] (excellent reliability ($0.75 > \text{ICC} \leq 1.00$), fair to good reliability ($0.40 \geq \text{ICC} \leq 0.75$), poor reliability ($0.00 \geq \text{ICC} \leq 0.40$). Statistical analyses were performed using SPSS, version 20 (IBM Corporation, Armonk, NY, USA).

Results

Inter- and intra-rater reliability of the mean T2 values is demonstrated with ICC values in Tables 2 and 3, respectively. Inter-rater reliability was excellent ($\text{ICC} > 0.75$) in every instance except for the posteromedial subregion viewed in the coronal plane ($\text{ICC} = 0.706$). Intra-rater reliability was excellent with the lower bound of the 95 % confidence interval of the ICC estimate exceeding 0.75 in all cases. There were four subjects, in which particular subregions did not include enough pixels to allow for a robust comparison between raters, and in this case, the regions were excluded for the ICC analysis.

Mean T2 values for each subregion are presented in Figs. 2 and 3. The lateral portion in the coronal plane well differentiated supraspinatus pathology. Using the coronal plane, the tear group (43.9 ± 12.7 ms) exhibited significantly higher mean T2 values in the anterolateral subregion than both the tendinosis (34.9 ± 3.9 ms; $p = 0.006$) and asymptomatic (33.6 ± 5.3 ms; $p = 0.015$) groups. Similarly, the tear group (45.2 ± 13.7 ms) had higher posterolateral mean T2 values than the asymptomatic group (34.7 ± 6.7 ms; $p = 0.012$). No statistically significant group differences were found in either the middle or medial subregions. Using the sagittal plane, the only significant difference was in the anteromedial subregion where the tendinosis group (43.6 ± 7.1 ms) had lower mean T2 values than the asymptomatic group (51.8 ± 9.7 ms; $p = 0.049$).

In nearly all cases where significant group differences existed, groups also had significantly different variability of values among subjects (as assessed by Levene's

Table 2 Inter-rater reliability in each subregion in the sagittal and coronal planes

Imaging plane	Subregion	*N*	Inter-rater reliability (ICC)	Lower bound	Upper bound
Sagittal	Lateral				
	A	46	0.902	0.829	0.944
	P	46	0.890	0.810	0.938
	Middle				
	A	49	0.783	0.645	0.872
	P	49	0.853	0.754	0.914
	Medial				
	A	49	0.853	0.753	0.914
	P	49	0.818	0.698	0.893
Coronal	Lateral				
	A	48	0.848	0.744	0.912
	P	47	0.838	0.727	0.907
	Middle				
	A	49	0.823	0.707	0.896
	P	48	0.809	0.683	0.888
	Medial				
	A	50	0.906	0.840	0.946
	P	49	0.706	0.532	0.823

A anterior, *P* posterior

Table 3 Intra-rater reliability in each subregion in the sagittal and coronal planes

Imaging plane	Subregion	*N*	Inter-rater reliability (ICC)	Lower bound	Upper bound
Sagittal	Lateral				
	A	47	0.954	0.919	0.974
	P	47	0.920	0.861	0.955
	Middle				
	A	50	0.948	0.910	0.970
	P	50	0.951	0.916	0.972
	Medial				
	A	50	0.920	0.863	0.954
	P	50	0.980	0.964	0.988
Coronal	Lateral				
	A	48	0.975	0.956	0.986
	P	46	0.956	0.922	0.975
	Middle				
	A	49	0.914	0.852	0.950
	P	47	0.928	0.874	0.959
	Medial				
	A	50	0.958	0.927	0.976
	P	48	0.985	0.974	0.992

A anterior, *P* posterior

homogeneity test). Commonly, standard deviations in mean T2 values were up to twice as high in the small (partial or minimally retracted full thickness) tear group.

Discussion

This study evaluated pathologic rotator cuff tendons using quantitative T2 mapping. Understanding and being able to measure quantitatively the process of tendon degeneration and subsequent tearing may help clinicians to better predict at-risk groups and to stratify treatment options. Our findings demonstrate that the lateral region in the coronal plane well differentiated supraspinatus tear pathology, with a significant difference between the asymptomatic versus small tear groups observed. There was a trend for a difference in the tendinosis group versus small tear group in the lateral region on the coronal plane; however, this did not reach

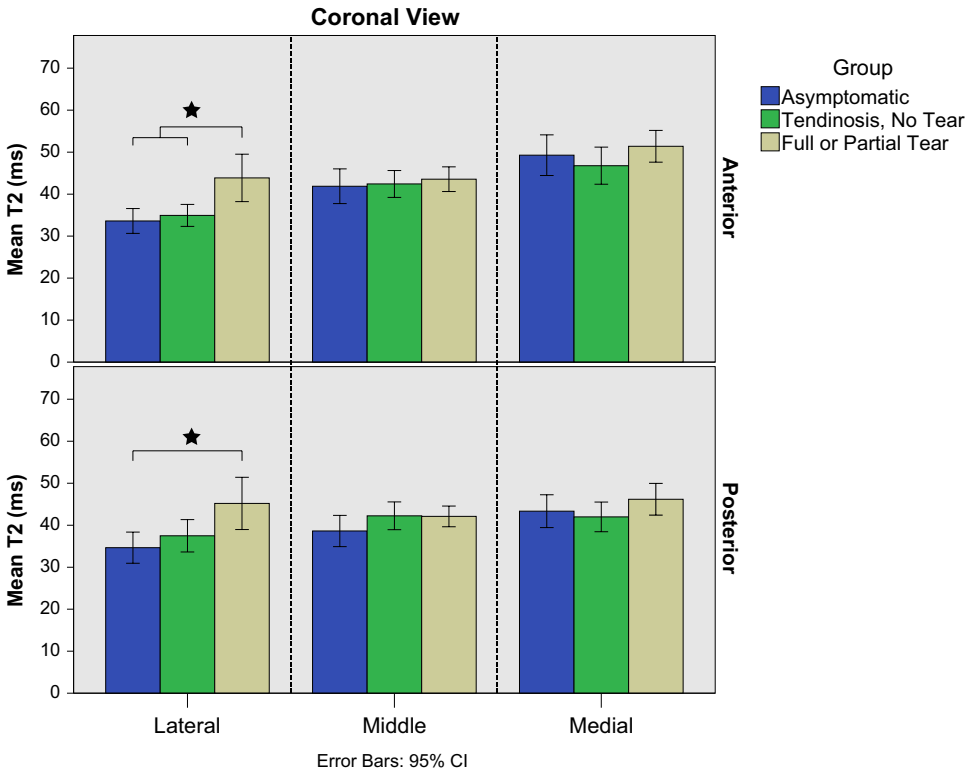

Fig. 2 Mean T2 values (ms) of asymptomatic, tendinosis, and partial or minimally retracted full-thickness tears in the coronal *plane*. *Stars* represent statistically significant ($p < 0.05$) group differences

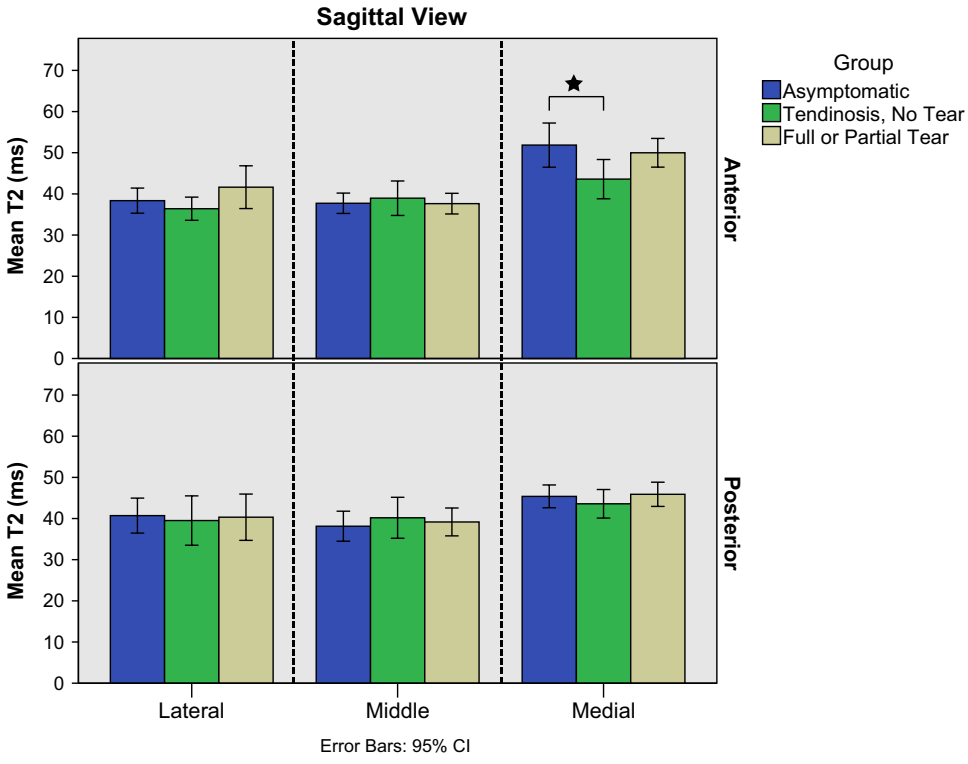

Fig. 3 Mean T2 values (ms) of asymptomatic, tendinosis, and partial or minimally retracted full-thickness tears in the sagittal *plane*. *Stars* represent statistically significant ($p < 0.05$) group differences

statistical significance. Commonly, SD in mean T2 values were up to twice as high in the small tear group, indicating greater variability in T2 values in patients presenting with arthroscopically verified tears. An unexpected finding was that in the anteromedial region, the tendinosis group had significantly lower T2 values than the asymptomatic group. This may be due to the range of tendinosis that is often seen clinically, and that is difficult to diagnose with conventional MRI. It is possible that both the tendinosis and asymptomatic groups in this study had a range of tendinosis present, making it difficult to differentiate between the two groups. Seven of the fifteen partial rotator cuff tears in our study were >50 % of the tendon thickness, which would further increase the difficulty of distinguishing between them. While conventional MRI can be used to identify discrete tears in the supraspinatus by the presence of a fluid-filled gap, T2 mapping presents the opportunity to look earlier and evaluate tissue quality degradation before the tear occurs. There is also the potential to identify the likelihood of tear progression, failure of healing, and re-tearing.

T2 values (also referred to as T2 relaxation times) are dependent on the rate at which nuclei lose phase coherence, and this is largely determined by water content and collagen orientation/disorder. This allows T2 mapping to assess soft tissue biomarkers for early tissue degeneration, particularly water content, collagen content, and collagen orientation [24, 35]. T2 mapping has been used to identify early degeneration in several types of soft tissues including articular cartilage [23], meniscus [34], and Achilles tendons [8]. To the best of our knowledge, our study is the first to use quantitative MRI in the assessment of rotator cuff pathology. We demonstrated the capability of T2 mapping to quantify degeneration associated with small or full-thickness tears of the rotator cuff which have proven historically difficult to diagnose using conventional MRI [2, 25, 27, 28]. This quantitative analysis is particularly useful for the rotator cuff, which has variable morphology and subjective signal change. As tendons degenerate, histologically there is a loss of cellularity, vascularity, tissue architecture, and fibrocartilaginous mass [21]. Decreased collagen content, particularly of type I collagen, has also been shown to occur [21]. With significant degeneration, there is a decrease in mechanical properties and increased risk of tearing. Histopathologic changes in rotator cuff tears occur not only at the site of rupture but also in the remaining intact rotator cuff tendon [16].

Muscle hypertrophy and fatty infiltration are observed in chronic, massive rotator cuff tears. Similar to tendon degeneration, muscle physiology, structure, and function are altered with rotator cuff tears. Myofibrils become disorganized, and the number and lengths of sarcomere are decreased [9]. Our study evaluated the supraspinatus tendon as a single muscle tendon unit rather than isolating the tendon alone in order to include early degenerative changes that occur in muscle and myotendon junction, primarily in the medial subregions. In a pilot evaluation, we observed no statistical difference in tendon-alone and muscle plus tendon unit T2 values in the medial, middle, and lateral subregions in either plane for all groups. Anz et al. [1] evaluated both the tendon-alone as well as the muscle and tendon unit using the same medial, middle, and lateral third subregions and noted no statistical difference between tendon-alone and tendon plus muscle T2 values in asymptomatic individuals. These authors reported excellent inter- and intra-rater reliability in all regions for both segmentation methods except in the tendon-alone segmentation medially where they found increased difficulty in identifying slips of tendon from muscle at the musculotendinous junction [1].

The data in this study suggest that manual segmentation is generalizable to future raters with excellent inter- and intra-rater reliability in all regions in both the coronal and sagittal planes except the posteromedial subregion viewed in the coronal plane (ICC = 0.706) which had "good" reliability. Although we found nearly all excellent reliability, there are some limitations with the ability to manually segment in the coronal and sagittal planes. In the sagittal plane, the lateral footprint was more difficult to segment manually due to tendon curvature and inherent partial volume averaging with the humerus from the MRI scan. Posterolaterally, the infraspinatus also curves anteriorly to insert on a trapezoidal region on the greater tuberosity and is covered by connective tissue [20] making isolation of the supraspinatus challenging at different anatomical locations in each plane. The authors preferred the coronal plane for the evaluation of the supraspinatus footprint and the sagittal plane for medial segmentation. An automatic segmentation algorithm and automated landmark detection are paramount for implementing the standard clinical protocol.

All patients received T2 mapping as part of their standard clinical MRI protocol. One strength of our study is that patients were enrolled in a prospective manner based on arthroscopic findings of supraspinatus pathology, and preoperative MRI T2 maps were then retrospectively manually segmented, reducing selection bias. These pathologic groups were also compared to a control asymptomatic group who were screened with physical exams and questionnaire. Another strength is that two observers of various training backgrounds (one musculoskeletal radiologist and one orthopaedic surgeon) each performed two manual segmentations separated by 30 days allowing for a robust assessment of inter- and intra-rater reliability.

One limitation of our study is that higher variability than expected was observed among patients with partial or small minimally retracted full-thickness tears. Consequently, a future larger study may be able to distinguish group differences that the current study was unable to detect including

a subgroup comparison of partial tears of both less than and greater than 50 % tendon thickness versus small full-thickness tears. This would aid in identifying a quantitative threshold for determining repair versus debridement of partial cuff tears. Another limitation is that we did not exclude patients from our study with other cuff pathology. Combined with difficulty isolating out the anterior part of the infraspinatus, T2 values may be falsely elevated in the posterior and lateral region if pathology also exists in the infraspinatus tendon. Also, we excluded full-thickness tears with retraction. Full-thickness tears with retraction would not allow for a robust subregional analysis. Therefore, our T2 values for the small tear group may not be as severe, since retracted tears are often larger with more degeneration and likely higher T2 values. We combined the small full-thickness tears with minimal retraction and the partial tears to enable viable comparison to the asymptomatic and tendinosis groups. The tendon properties and T2 values for partial tears and for small full-thickness tears may not be substantially different, but this remains to be documented and is a limitation. In the future, it would be ideal to obtain tissue biopsies from each patient to correlate tissue degeneration histologically with areas of increased T2 values, but this of course would require IRB evaluation and may not be practical.

The results of the present study may set the groundwork for several future studies. The ability to evaluate tendon degeneration quantitatively and non-invasively can be used to evaluate the natural history of rotator cuff pathology in both symptomatic and asymptomatic individuals, longitudinally. Identifying a threshold of tendon degeneration when tears progress or become symptomatic would be valuable in counselling patients of their prognosis and treatment options and formulating a treatment algorithm. Pre-operative T2 mapping of tears with relatively lower T2 values may be a good prognostic indicator and may be used to better counsel patients. Response to treatment could also be quantitatively measured, and the normalization of the T2 mapping score could help clinicians to determine a more objective measure of when it would be safe to progress rehabilitation or return to activities. Furthermore, since qualitative MRI information such as fatty infiltration and muscle atrophy has been shown to correlate with increased re-tear rates and poor patient outcomes [15], prognosis could significantly improve with earlier detection and intervention. For 50 and 75 % partial articular-sided tears, biomechanical studies have demonstrated increased strain on the remaining tendon [19], and surgical decision-making regarding repair versus debridement for partial rotator cuff tears based on a pre-operative objective measure of tissue degeneration could lead to earlier surgical intervention and improved outcomes. Conventional MRI is also variable in identifying rotator cuff re-tear after repair [10], but T2 mapping may allow a more accurate assessment of healing by detecting changes in T2 values. Cell-based therapies aimed at halting or reversing the degenerative process at a cellular and molecular level and biologic augmentation to current repair techniques are of recent interest [3], and T2 mapping would allow a non-invasive quantitative method to assess these results.

Conclusion

In conclusion, T2 mapping was found to be an accurate non-invasive imaging technique to identify quantitatively early rotator cuff pathology in this study. More specifically, the lateral region in the coronal plane can differentiate partial and full-thickness tears from tendinosis and normal supraspinatus tendons. Furthermore, the methodology presented, including the subregions used for analysis, is generalizable to future raters as excellent inter- and intra-rater reliability in all regions and degrees of pathology in both the coronal and sagittal planes was found. This method has myriad clinical applications for those interested in studying the natural history and clinical course of rotator cuff disease. Understanding and being able to measure quantitatively the process of tendon degeneration and subsequent tearing may help clinicians to better predict at-risk groups and to stratify treatment options.

Acknowledgments Funding for this study came from the internal institution Steadman Philippon Research Institute, where the research was performed. None of the authors have a conflict of interest related to the subject of this article.

Ethical standard All procedures performed in studies involving human participants were in accordance with the ethical standards of the institutional and/or national research committee and with the 1964 Helsinki Declaration and its later amendments or comparable ethical standards.

Informed consent Informed consent was obtained from all individual participants included in the study. This study was approved by the Institutional Review Board at Steadman Philippon Research Institute, and the approved protocol number is 2012–2007.

References

1. Anz AW, Lucas EP, Fitzcharles EK, Surowiec RK, Millett PJ, Ho CP (2014) MRI T2 mapping of the asymptomatic supraspinatus tendon by age and imaging plane using clinically relevant subregions. Eur J Radiol 83(5):801–805
2. Balich SM, Sheley RC, Brown TR, Sauser DD, Quinn SF (1997) MR imaging of the rotator cuff tendon: interobserver agreement and analysis of interpretive errors. Radiology 204:191–194
3. Bedi A, Maak T, Walsh C, Rodeo SA, Grande D, Dines DM, Dines JS (2012) Cytokines in rotator cuff degeneration and repair. J Shoulder Elb Surg 21:218–227

4. Bryant L, Shnier R, Bryant C, Murrell GA (2002) A comparison of clinical estimation, ultrasonography, magnetic resonance imaging and arthroscopy in determining the size of rotator cuff tears. J Shoulder Elb Surg 11:219–224
5. Buck FM, Grehn H, Hilbe M, Pfirrmann CW, Manzanell S, Hodler J (2010) Magnetic resonance histologic correlation in rotator cuff tendons. J Magn Reson Imaging 32:165–172
6. Fleiss JL (1986) The design and analysis of clinical experiments. Wiley, New York
7. Juras V, Apprich S, Pressl C, Zbyn S, Szomolanyi P, Domayer S, Hofstaetter JG, Trattnig S (2013) Histological correlation of 7 T multi-parametric MRI performed in ex vivo Achilles tendon. Eur J Radiol 82:740–744
8. Juras V, Zbyn S, Pressl C, Valkovic L, Szomolanyi P, Frollo I, Trattnig S (2012) Regional variations of T2* in healthy and pathologic achilles tendon in vivo at 7 Tesla: preliminary results. Magn Reson Med 5:1607–1613
9. Kang JR, Gupta R (2012) Mechanisms of fatty degeneration in massive rotator cuff tears. J Shoulder Elb Surg 21:175–180
10. Khazzam M, Kuhn JE, Mulligan E, Abboud JA, Baumgarten KM, Brophy RH, Jones GL, Miller B, Smith M, Wright RW (2012) Magnetic resonance imaging identification of rotator cuff retears after repair: interobserver and intraobserver agreement. Am J Sports Med 40:1722–1727
11. Kijowski R, Blankenbaker DG, Munoz Del Rio A, Baer GS, Graf BK (2013) Evaluation of the articular cartilage of the knee joint: value of adding a T2 mapping sequence to a routine MR imaging protocol. Radiology 267:503–513
12. Kim M, Dahiya N, Teefey SA, Middleton WD, Stobbs G, Steger-May K, Yamaguchi K, Keener JD (2010) Location and initiation of degenerative rotator cuff tears. J Bone Joint Surg Am 92:1088–1096
13. Kim T, Min BH, Yoon SH, Kim H, Park S, Lee HY, Kwack KS (2014) An in vitro comparative study of T2 and T2* mappings of human articular cartilage at 3-Tesla MRI using histology as the standard of reference. Skelet Radiol 43:947–954
14. Lattanzi R, Petchprapa C, Ascani D, Babb JS, Chu D, Davidovitch RI, Youm T, Meislin RJ, Recht MP (2014) Detection of cartilage damage in femoroacetabular impingement with standardized dGEMRIC at 3 T. Osteoarthr Cartil 22:447–456
15. Liem D, Lichtenberg S, Magosch P, Habermeyer P (2007) Magnetic resonance imaging of arthroscopic supraspinatus tendon repair. J Bone Joint Surg Am 89:1770–1776
16. Longo UG, Franceschi F, Ruzzini L, Rabitti C, Morini S, Maffulli N, Denaro V (2008) Histopathology of the supraspinatus tendon in rotator cuff tears. Am J Sports Med 36:533–538
17. Malhi AM, Khan R (2005) Correlation between clinical diagnosis and arthroscopic findings of the shoulder. Postgrad Med J 81:657–659
18. Matsen FA III, Arntz CT, Lippitt SB (1998) Rotator Cuff. In: Rockwood CA, Matsen FA III (eds) The shoulder, 2nd edn. Saunders, Philadelphia, pp 755–839
19. Mazzocca AD, Rincon LM, O'Connor RW, Obopilwe E, Anderson M, Geaney L, Arciero RA (2008) Intra-articular partial-thickness rotator cuff tears: analysis of injured and repaired strain and behavior. Am J Sports Med 36:110–116
20. Mochizuki T, Sugaya H, Uomizu M, Maeda K, Matsuki K, Sekiya I, Muneta T, Akita K (2008) Humeral insertion of the supraspinatus and infraspinatus. J Bone Joint Surg Am 90:962–969
21. Nho SJ, Yadav H, Shindle MK, MacGillivray JD (2008) Rotator cuff degeneration: etiology and pathogenesis. Am J Sports Med 36:987–993
22. Nishioka H, Hirose J, Nakamura E, Okamoto N, Karasugi T, Taniwaki T, Okada T, Yamashita Y, Mizuta H (2013) Detecting ICRS grade 1 cartilage lesions in anterior cruciate ligament injury using T1rho and T2mapping. Eur J Radiol 82:1499–1505
23. Nishioka H, Hirose J, Nakamura E, Oniki Y, Takada K, Yamashita Y, Mizuta H (2012) T1ρ and T2 mapping reveal the in vivo extracellular matrix of articular cartilage. J Magn Reson Imaging 35:147–155
24. Nissi MJ, Töyräs J, Laasanen MS, Rieppo J, Saarakkala S, Lappalainen R, Jurvelin JS, Nieminen MT (2004) Proteoglycan and collagen sensitive MRI evaluation of normal and degenerated articular cartilage. J Orthop Res 22:557–564
25. Ostör AJ, Richards CA, Tytherleigh-Strong G, Bearcroft PW, Prevost AT, Speed CA, Hazleman BL (2013) Validation of clinical examination versus magnetic resonance imaging and arthroscopy for the detection of rotator cuff lesions. Clin Rheumatol 32:1283–1291
26. Patte D (1990) Classification of rotator cuff lesions. Clin Orthop Relat Res 254:81–86
27. Reinus WR, Shady KL, Mirowitz SA, Totty WG (1995) MR diagnosis of rotator cuff tears of the shoulder: value of using T2-weighted fat-saturated images. Am J Roentgenol 164:1451–1455
28. Robertson PL, Schweitzer ME, Mitchell DG, Schlesinger F, Epstein RE, Frieman BG, Fenlin JM (1995) Rotator cuff disorders: interobserver and intraobserver variation in diagnosis with MR imaging. Radiology 194:831–835
29. Spencer EE, Dunn WR, Wright RW, Wolf BR, Spindler KP, McCarty E, Ma CB, Jones G, Safran M, Holloway GN, Kuhn JE (2008) Interobserver agreement in the classification of rotator cuff tears using magnetic resonance imaging. Am J Sports Med 36:99–103
30. Takamiya H, Kusaka Y, Seo Y, Noguchi M, Ikoma K, Morimoto T, Hirasawa Y (2000) Characteristics of proton NMR T(2) relaxation of water in the normal and regenerating tendon. Jpn J Physiol 50:569–576
31. Teefey SA, Rubin DA, Middleton WD, Hildebolt CF, Leibold RA, Yamaguchi K (2004) Detection and quantification of rotator cuff tears. comparison of ultrasonographic, magnetic resonance imaging, and arthroscopic findings in seventy-one consecutive cases. J Bone Joint Surg Am 86-A:708–716
32. Vitale MA, Vitale MG, Zivin JG, Braman JP, Bigliani LU, Flatow EL (2007) Rotator cuff repair: an analysis of utility scores and cost-effectiveness. J Shoulder Elb Surg 16(2):181–187
33. Watrin-Pinzano A, Ruaud JP, Olivier P, Grossin L, Gonord P, Blum A, Netter P, Guillot G, Gillet P, Loeuille D (2005) Effect of proteoglycan depletion on T2 mapping in rat patellar cartilage. Radiology 234:162–170
34. Williams A, Qian Y, Golla S, Chu CR (2012) UTE-T2* mapping detects sub-clinical meniscus injury after anterior cruciate ligament tear. Osteoarthr Cartil 20:486–494
35. Yao W, Qu N, Lu Z, Yang S (2009) The application of T1 and T2 relaxation time and magnetization transfer ratios to the early diagnosis of patellar cartilage osteoarthritis. Skelet Radiol 38:1055–1062